1   ## CD5 expressing CD8^{+} T cell subsets differ between children with Type 1

2   ## Diabetes and controls

3

4   Josefine Wadenpohl[1], Julia Seyfarth[1], Paul Hehenkamp[1], Maximilian Hoffmann[1], Sebastian

5   Kummer[1], Christina Reinauer[1], Carsten Döing[1], Katharina Förtsch[1], Ertan Mayatepek[1],

6   Thomas Meissner[1], Marc Jacobsen[1*]

7

8   [1] Department of General Pediatrics, Neonatology and Pediatric Cardiology, University

9   Children's Hospital, Medical Faculty and University Hospital Düsseldorf, Heinrich-Heine-

10   University Düsseldorf, Germany

11

12

13

14

15

16

17

18   [*] **Correspondence:**

19   Prof. Dr. Marc Jacobsen

20   Department of General Pediatrics, Neonatology, and Pediatric Cardiology

21   University Children's Hospital, Moorenstr. 5

22   40225 Duesseldorf, Germany

23   Phone:++49(211) 81-16623

24   Email: marc.jacobsen@med.uni-duesseldorf.de

1 **Abstract**

2 Different lymphocyte subsets are involved in autoimmune pathogenesis of Type 1 Diabetes

3 (T1D). Previous studies suggested a role of CD5 expressing T and B cells including rare

4 unconventional lymphocytes with combined T- and B-cell features (DE cells). We performed

5 algorithm-supported multi-parameter flow cytometry and quantitative PCR to investigate

6 immune cell subsets and DE cells in children with T1D (n=20) and matched controls (n=20).

7 Comparisons of conventional immune cells detected increased proportions of CD3+ T cells in

8 T1D patients whereas CD19+ B cell proportions were comparable to controls. Self-organizing

9 maps for flow cytometry analyses (FlowSOM) showed highly similar CD5 expressing B-cell

10 subsets and no differences for DE cells were detected between the study groups by flow

11 cytometry or specific quantitative PCR. Notably, differences in CD8 positive T cells were

12 indicated by FlowSOM and similarity-based tSNE analyses. Study group comparison confirmed

13 significantly reduced CD8+ T-cell proportions with moderate or low CD5 expression in T1D

14 patients. Finally, *In vitro* experiments showed stable CD5 expression differences of CD8+ T cells

15 after T-cell activation, cytokine stimulation and culture.

16 We observed differences of T-cell co-receptor CD5 expression in T1D patients with potential

17 relevance for immune regulation of CD8+ T-cell activation.

1 **Introduction**

2 CD5 is a membrane receptor expressed on the vast majority of T cells and a minor subset of B

3 cells in humans. As part of the T-cell receptor signaling complex, CD5 is recruited to the

4 immunological synapse and contributes to T-cell receptor signal regulation after activation (1).

5 Whereas initial studies described co-stimulatory efficacy of CD5, more recent studies from

6 animal models demonstrated inhibitory effects of CD5 on T-cell activation (2). CD5 is involved

7 in the regulation of thymic lymphocyte selection (3) as well as mature T-cell functions

8 including tolerance induction by dendritic cells (4) and activation induced cell death (5). A

9 potential role of CD5^{+} T cells in the pathogenesis of autoimmune diseases has been described

10 (5; 6). In B cells, CD5 expression characterizes a subset with regulatory function (7). These IL-

11 10 producing B cells play a crucial role in different autoimmune diseases including Type 1

12 Diabetes (T1D) (8-10). B and T cells are involved in immune pathology of T1D and especially

13 self-reactive T cells contribute to the destruction of insulin producing pancreatic β-cells.

14 Insulin autoantigens are important targets in T1D and, recently, a non-conventional immune

15 cell subset with both, T- and B-cell features, has been found in T1D patients (11). This cell type

16 expresses CD19 together with CD5 and a unique IgD antibody coding for a superagonist

17 clonotype recognized by insulin-specific T cells (11). Because of concomitant T-cell receptor

18 α/β chain expression, these cells were termed 'dual expressing' (DE) cells and initial

19 comparisons revealed higher DE cell proportions in T1D patients as compared to controls (11).

20 Previous reports indicated distinct roles of $CD5_{high}$ or $CD5_{low}$ immune cell populations in

21 immunopathologies and, hence, we investigated CD5 in combination with B- and T-cells

22 markers in T1D patients and matched controls using algorithm supported multi-color flow

23 cytometry and quantitative PCR. Multiple immune cell populations were compared between

24 study groups and dimensionality reduction tools together with flowcytometry based self-

25 organizing maps (FlowSOM) were applied to identify novel populations and differences in CD5

26 expressing immune cell subsets.

1 **Methods**

2 **Donor Characteristics**

3 We recruited children with Type 1 Diabetes (T1D patients, n=20) and healthy children

4 (Controls, n=20) at University Children´s Hospital, Duesseldorf, Germany. Both study groups

5 had similar distributions of age (T1D: 11.9 ± 2.8; controls: 11.7 ± 5.1) and sex (T1D: 50% males;

6 controls: 55% males). T1D patients had a mean disease duration of 5.4 years (± 3.3 years).

7 Controls had a negative history for autoimmune and systemic autoinflammatory diseases. For

8 *in vitro* experiments six healthy adult individuals were recruited. The present study was

9 approved by the Ethical Committee of the Medical Faculty of Heinrich-Heine-University

10 Duesseldorf, Germany (ID 2019-423). Written informed consent was received from legal

11 guardians of all donors, and from donors if older than 14 years.

12

13 **Phenotyping of PBMC subset by flow cytometry**

14 Heparinized venous blood (10ml) was taken from each participant and PBMCs were isolated

15 by density centrifugation (Ficoll, Biochrom, Berlin, Germany) according to manufacturer´s

16 instructions and stored in liquid nitrogen. 10 samples (5 from each study group) were

17 concomitantly processed for phenotyping. PBMC were stained with antibodies against human

18 CD3-PerCP-Cy5.5, CD4-BV510, CD5-PE-Cy7, CD8-V450, CD19-BV786, CD45RA-FITC, CD45RO-

19 PE-CF594, IgD-APC, and TCRα/β-PE (all Biolegend). Fixable viability dye eFlour780 (Thermo

20 Fisher Scientific) was applied to exclude dead cells. All samples were stained in triplicates.

21 Measurements were performed on a LSR Fortessa flow cytometer (BD Biosciences). The

22 investigator was blinded with regard to group allocation when measuring the samples.

23 Data analysis has been performed using FlowJo software (version 10; Miltenyi Biotech). The

24 following steps were performed for i) algorithm supported identification of cell populations

25 (i.e. FlowSOM, see below), ii) complexity reduction tools (i.e. t-SNE, TriMap, see below), iii)

1 quantification of immune cell populations for individual donors. For gating strategy see

2 Supplementary Figure 1. For combined analyses, viable cells were downsampled to 1.000 cells

3 per donor using the Downsample v3.3 plugin for FlowJo and were concatenated to one sample

4 per group. Complexity reduction was performed on all samples concomitantly whereas

5 FlowSOM was done for each study group separately.

6

7 **Complexity reduction tools: t-SNE and TriMAP analysis**

8 Both, t-distributed Stochastic Neighbor Embedding (t-SNE) and TriMap calculate two-

9 dimensional depiction of multi-factorial similarity (12; 13). The proximity of cells is illustrated

10 by their distances in the respective graphs. t-SNE calculations were performed as described

11 (14). TriMap analysis was performed using the FlowJo TriMap 0.2 plugin downloaded from

12 www.flowjo.com/exchange/. Default settings were applied including the euclidean distance

13 function, a number of ten nearest neighbours, and five outliers. Zebra and dot plots were

14 generated for t-SNE and TriMap calculations.

15

16 **FlowSOM algorithm**

17 After concatenation, cells from both study groups were separately gated and processed using

18 the FlowSOM (Flow cytometry Self Organizing Maps) algorithm. The number of clusters was

19 set to six (for B-cell subset analysis) or to seven (for T-cell subsets). The SOM grid was set to 7

20 x 7. All other parameters were left at manufacturer's default settings. For the second study

21 group, we choose the option 'apply on map' of the first analyzed study group. Heat maps were

22 generated for both study groups including all parameters.

23

24 **Quantitative PCR analyses**

1 qPCR analyses have been done as described (15) using GAPDH as a housekeeping gene and

2 the following primer pairs for the B-cell receptor variable β-chain (VDJ;

3 forw.:TCCAAGAACCAGTTCTCCCTG; rev.:CTGGCCCCAGTAGTCAAAGTAG) and the DE cell

4 complementary determining region (x-clonotype; forw.:TCCAAGAACCAGTTCTCCCTG;

5 rev.:AGCTGTATCCTCCTGTCTCG) as described (11).

6

7 *In vitro* **T-cell activation**

8 Cryopreserved PBMC were cultured in X-vivo15 medium (Lonza) supplemented with L-

9 Glutamine (2mM, Sigma-Aldrich) and Penicllin/Streptomycin (50U/ml, Sigma-Aldrich) at a

10 concentration of 2 x 10^5 cells per round-bottom well and stimulated for 96h with CD3/CD28

11 dynabeads (0.2μl/well; Thermofisher), Interleukin-7 (IL-7, 10ng/ml, Sigma-Aldrich) or left

12 unstimulated. Afterwards cells were stained with antibodies and measured by flow cytometry

13 as described above.

14

15 **Calculations and statistics**

16 Graph Pad Prism 9 (Version 9.0.0, GraphPad Software, La Jolla, CA) software was used for

17 statistical analyses and preparation of graphs. Because of moderate study group sizes non-

18 parametric distributions were assumed and the non-parametric Mann-Whitney U-test (two-

19 tailed) was used for study group comparisons.

1   **Results**

2   Autoantigen specific CD19+ B cells and CD3+ T cells play central roles in T1D pathogenesis.

3   Hence, we initially compared total B- and T-cell proportions between the study groups.

4   Whereas frequencies of B cells showed no differences, we identified significantly higher T-cell

5   proportions in T1D patients as compared to controls (Figure 1a). Next, we characterized B-cell

6   subsets using a dimensional reduction tool for multi-factorial flow cytometry analyses (tSNEt)

7   of patients with T1D and matched controls (Figure 1a). CD19+ B cells clustered in the same

8   region of tSNE graphs between the study groups (Figure 1b, upper plots) and also the

9   distribution of IgD expressing naïve B cells showed no obvious differences (Figure 1b, middle

10 plots). Moreover CD5, a marker of regulatory B cells, was expressed on comparable subsets

11 of T1D patients and controls (Figure 1b, lower plots). Next, we applied self organizing maps

12 software (FlowSOM) to identify subpopulations within CD19+ cells on the basis flow cytometry

13 markers. Heat map depiction for a defined number of six populations (B_0 to B_5) showed high

14 similarity between T1D patients and controls for all included markers (Figure 1c). To validate

15 this, we compared B-cell subset proportions between individuals from both study groups. No

16 differences in IgD+ naïve/IgD+ memory B cells were detected (Figure 1d) and CD5+ or negative

17 B-cell proportions were comparable between T1D patients and controls (Figure 1e). These

18 results did not suggest differences in CD19+/CD5+ B-cell proportions between T1D patients

19 and controls. Next, DE cells (CD19+/CD5+/IgD+/TCR$\alpha\beta$+) were analyzed (for gating strategy see

20 Supplementary Figure 1). We detected DE cells at generally low proportions but no differences

21 between T1D patients and controls (Figure 1f). Quantitative PCR analyses of DE-specific

22 clonotypic IgD receptor (i.e. complementary determing region, CDR3) and for the described

23 variable (VDJ) heavy chain (11) found a tendency of higher VDJ region expression in T1D

24 patients but no differences for the clonotype CDR3 between the study groups (Figure 1g).

1   CD5 is also expressed on the majority of T cells and we detected significant higher T-cell

2   proportions in T1D patients (Figure 1a). Therefore, we next performed FlowSOM analysis to

3   compare T-cell subsets based on the expression of multiple markers (Figure 2a). Three T-cell

4   subsets CD4$^+$, CD8$^+$, and double-negative (DN; CD3$^+$/CD4$^-$/CD8$^-$) T cells were classified.

5   Interestingly, only CD8$^+$ T cells showed differences in marker expression pattern between the

6   study groups (Figure 2a). Two of three CD8$^+$ subsets showed typical features of naïve and

7   memory T cells, respectively. The third subset, however, had intermediate CD45RA and low

8   CD45RO expression and showed differences in CD5 expression levels between the study

9   groups (Figure 2a). The heatmap indicated low CD5 expression of this CD8$^+$ T-cell subset in

10 controls whereas medium CD5 expression characterized this subset in children with T1D.

11 To further analyze CD8$^+$ with differential CD5 expression, we applied TriMAP, an efficient

12 diversity reduction algorithm that depicts cell phenotype similarities based on two calculated

13 parameters (see Methods). Concatenated data sets (combined for all individuals within each

14 study group) were applied. Highlighted CD8$^+$ CD5$_{high}$ and CD5$_{low}$ T-cell subsets in zebra plots

15 suggested differences in CD8$^+$/CD5$_{low}$ cells between the study groups (Figure 2b). Proportional

16 differences were confirmed by gating of CD8$^+$ T cells with CD5$_{low}$, CD5$_{medium}$ and CD5$_{high}$

17 expression (Figure 2c). CD5$_{low}$ and CD5$_{medium}$ CD8$^+$ T cells were more frequent in controls

18 whereas CD5$_{high}$ CD8$^+$ T cells were more frequent in T1D patients (Figure 2c). We next

19 compared CD8/CD5 T-cell subset between individual donors from both study groups (Figure

20 2d). Analyses confirmed the algorithm prediction and detected significantly lower CD5$_{medium}$

21 and CD5$_{low}$ CD8$^+$ T-cell proportions in T1D patients as compared to controls whereas CD5$_{high}$

22 cells were more frequent in T1D patients (Figure 2d).

23 We detected low or medium CD5 expression on subsets of CD8$^+$ T cells predominantly in

24 controls. To address the question if these subsets are functional T cells, we performed *in vitro*

25 stimulation of T cells from six healthy adult donors (HC1 – HC6). *Ex vivo* T-cell phenotyping

1   detected variable proportions of CD8$^+$ subsets with differential CD5 expression in individual

2   donors (Figure 3a; upper panel). Notably, after culture for 96h, proportions of CD5$_{low}$,

3   CD5$_{medium}$, and CD5$_{high}$ CD8$^+$ T cells hardly changed and donors with relatively high proportions

4   of CD5$_{medium}$ (i. e. HC3, HC5) or CD5$_{low}$ (i. e. HC3, HC6) cells still showed a similar pattern (Figure

5   3a; upper panel). Since dead cells were excluded from analyses, these results indicated that

6   CD5$_{medium}$ and CD5$_{low}$ CD8$^+$ T cells survived *in vitro* culture. Finally, we added T-cell activator

7   (CD3/CD28-coated beads) and/or the T-cell survival factor Interleukin-7 (IL-7) to culture

8   samples. Both, IL-7 and the T-cell activator, strongly induced proliferation and T-cell blasting

9   (data not shown) but CD5$_{low}$ and CD5$_{medium}$ CD8$^+$ T cells were still detectable after 96h (Figure

10   3b). The sample number was too small to detect significant differences between the

11   conditions, however, especially in donors with high CD5$_{medium}$ and CD5$_{low}$ proportions these

12   subsets tended to decrease during T-cell stimulation and also in the presence of IL-7 (Figure

13   3b).

1   **Discussion**

2   We applied a powerful approach including a combination of multi-parameter flow cytometry,

3   dimensionality reduction tools and self-organizing maps to compare immune cell

4   subpopulations between T1D patients and controls. This way, we identified CD8+ T-cell subsets

5   characterized by differential CD5 expression and proportional differences between the study

6   groups. Decreased CD5 expression of CD8+ T cells has been described before and was

7   associated with aberrant T-cell activation e. g. under inflammatory conditions (16). This was

8   in accordance with the described role of CD5 as co-inhibitory receptor (1). Others described

9   an important role of CD5 in the induction of activation-induced apoptosis (5). This group

10   demonstrated that CD5 knock-out prevented the development of experimental autoimmune

11   encephalomyelitis (EAE), the animal model of multiple sclerosis (5; 6). Here, we show that low

12   CD5 is found on a subset of CD8+ T cells in healthy individuals. Interestingly, animal knock-

13   down experiments suggested a role of CD5 during physiological selection of natural regulatory

14   T cells (nTregs) in the thymus (17). In the absence of CD5 increased proportions of fully

15   functional mature nTregs were found suggesting nTregs independency from CD5 mediated

16   co-stimulation (17). Moreover, CD5 signalling was shown to inhibit Treg function (18). Given

17   the fact that $CD5_{low}$ and $CD5_{medium}$ CD8+ T cells are rare in T1D, one may speculate about a

18   protective – potential regulatory – role of these CD8+ T cells against T1D as described for EAE

19   (19). In this regard efforts to treat T1D patients with anti-CD5 drugs (2) may preferentially

20   deplete effector T cells but not Tregs. A combination of Treg supporting treatment strategies

21   (e. g. low-dose IL-2) with CD5 depleting drugs could therefore be a favourable approach.

22   Future studies will have to characterize the underlying mechanism of decreased CD5

23   expression of CD8+ T cells.

1 **Acknowledgments**

1   **References**

2   1. Brossard C, Semichon M, Trautmann A, Bismuth G: CD5 inhibits signaling at the

3   immunological synapse without impairing its formation. J Immunol 2003;170:4623-4629

4   2. Consuegra-Fernandez M, Aranda F, Simoes I, Orta M, Sarukhan A, Lozano F: CD5 as a Target

5   for Immune-Based Therapies. Crit Rev Immunol 2015;35:85-115

6   3. Tarakhovsky A, Kanner SB, Hombach J, Ledbetter JA, Muller W, Killeen N, Rajewsky K: A role

7   for CD5 in TCR-mediated signal transduction and thymocyte selection. Science 1995;269:535-

8   537

9   4. Hawiger D, Masilamani RF, Bettelli E, Kuchroo VK, Nussenzweig MC: Immunological

10   unresponsiveness characterized by increased expression of CD5 on peripheral T cells induced

11   by dendritic cells in vivo. Immunity 2004;20:695-705

12   5. Axtell RC, Webb MS, Barnum SR, Raman C: Cutting edge: critical role for CD5 in experimental

13   autoimmune encephalomyelitis: inhibition of engagement reverses disease in mice. J

14   Immunol 2004;173:2928-2932

15   6. Axtell RC, Xu L, Barnum SR, Raman C: CD5-CK2 binding/activation-deficient mice are

16   resistant to experimental autoimmune encephalomyelitis: protection is associated with

17   diminished populations of IL-17-expressing T cells in the central nervous system. J Immunol

18   2006;177:8542-8549

19   7. Yanaba K, Bouaziz JD, Haas KM, Poe JC, Fujimoto M, Tedder TF: A regulatory B cell subset

20   with a unique CD1dhiCD5+ phenotype controls T cell-dependent inflammatory responses.

21   Immunity 2008;28:639-650

22   8. Deng C, Xiang Y, Tan T, Ren Z, Cao C, Huang G, Wen L, Zhou Z: Altered Peripheral B-

23   Lymphocyte Subsets in Type 1 Diabetes and Latent Autoimmune Diabetes in Adults. Diabetes

24   Care 2016;39:434-440

1   9. Saxena A, Yagita H, Donner TW, Hamad ARA: Expansion of FasL-Expressing CD5(+) B Cells in

2   Type 1 Diabetes Patients. Frontiers in immunology 2017;8:402

3   10. De Filippo G, Pozzi N, Cosentini E, Cavalcanti M, Carel JC, Tamasi S, Franzese A, Pignata C:

4   Increased CD5+CD19+ B lymphocytes at the onset of type 1 diabetes in children. Acta Diabetol

5   1997;34:271-274

6   11. Ahmed R, Omidian Z, Giwa A, Cornwell B, Majety N, Bell DR, Lee S, Zhang H, Michels A,

7   Desiderio S, Sadegh-Nasseri S, Rabb H, Gritsch S, Suva ML, Cahan P, Zhou R, Jie C, Donner T,

8   Hamad ARA: A Public BCR Present in a Unique Dual-Receptor-Expressing Lymphocyte from

9   Type 1 Diabetes Patients Encodes a Potent T Cell Autoantigen. Cell 2019;177:1583-1599 e1516

10 12. Mair F, Hartmann FJ, Mrdjen D, Tosevski V, Krieg C, Becher B: The end of gating? An

11 introduction to automated analysis of high dimensional cytometry data. Eur J Immunol

12 2016;46:34-43

13 13. Warmuth MKA, E.: TriMap: Large-scale dimensionality reduction using triplets. arXiv

14 2019;[preprint] 1910.00204

15 14. Seyfarth J, Mutze N, Antony Cruz J, Kummer S, Reinauer C, Mayatepek E, Meissner T,

16 Jacobsen M: CD4(+) T-Cells With High Common gamma Chain Expression and Disturbed

17 Cytokine Production Are Enriched in Children With Type-1 Diabetes. Frontiers in immunology

18 2019;10:820

19 15. Lundtoft C, Afum-Adjei Awuah A, Rimpler J, Harling K, Nausch N, Kohns M, Adankwah E,

20 Lang F, Olbrich L, Mayatepek E, Owusu-Dabo E, Jacobsen M: Aberrant plasma IL-7 and soluble

21 IL-7 receptor levels indicate impaired T-cell response to IL-7 in human tuberculosis. PLoS

22 pathogens 2017;13:e1006425

23 16. Wada T: Downregulation of CD5 and dysregulated CD8(+) T-cell activation. Pediatr Int

24 2018;60:776-780

17. Ordonez-Rueda D, Lozano F, Sarukhan A, Raman C, Garcia-Zepeda EA, Soldevila G: Increased numbers of thymic and peripheral CD4+ CD25+Foxp3+ cells in the absence of CD5 signaling. European journal of immunology 2009;39:2233-2247

18. Dasu T, Qualls JE, Tuna H, Raman C, Cohen DA, Bondada S: CD5 plays an inhibitory role in the suppressive function of murine CD4(+) CD25(+) T(reg) cells. Immunology letters 2008;119:103-113

19. Abdalla AE, Lambert N, Duan X, Xie J: Interleukin-10 Family and Tuberculosis: An Old Story Renewed. Int J Biol Sci 2016;12:710-717

1 **Legends to figures**

2 ***Figure 1: B-cell subset and DE-cell distribution in T1D patients and controls.*** Immune cell

3 phenotyping of peripheral blood by flow cytometry is shown as violin plots for CD3$^+$ T cells

4 and CD19$^+$ B cells. B-cell subtyping is depicted as comparison of individual donors (violin plots;

5 **d, e, f, g**), t-SNE similarity plots (**b**), and FlowSOM heatmaps (**c**). t-SNE plots are generated

6 using a concatenated data set from viable cell subsets of all individuals (down-sampled 1000

7 cells per donor sample; triplicate measures per donor were performed). Each dot represents

8 a cell and proximity of dots is a measure of similarity. CD19$^+$ as well as CD19$^+$/IgD$^+$ and

9 CD19$^+$/CD5$^+$ are highlighted by indicated colors (**b**). FlowSOM analyses were performed using

10 gated CD19$^+$ B cells of T1D patients and control children separately after concatenation. Six

11 clusters were chosen arbitrarily and respective clusters (B$_0$ to B$_5$) are shown for both study

12 groups (**c**). (**a, d, e, f, g**) Violin plots indicate median, 25-, and 75-percentile values as dotted

13 or dashed lines. (**g**) DE cell B-cell receptor (VDJ) and clonotype (CDR3) specific quantitative

14 PCR results are shown for both study groups as violin plots**.** The two-tailed Mann Whitney U-

15 test was performed and nominal p-values are given if comparisons are significant or show a

16 trend. 20 T1D patients and 20 controls were included and triplicate measures were
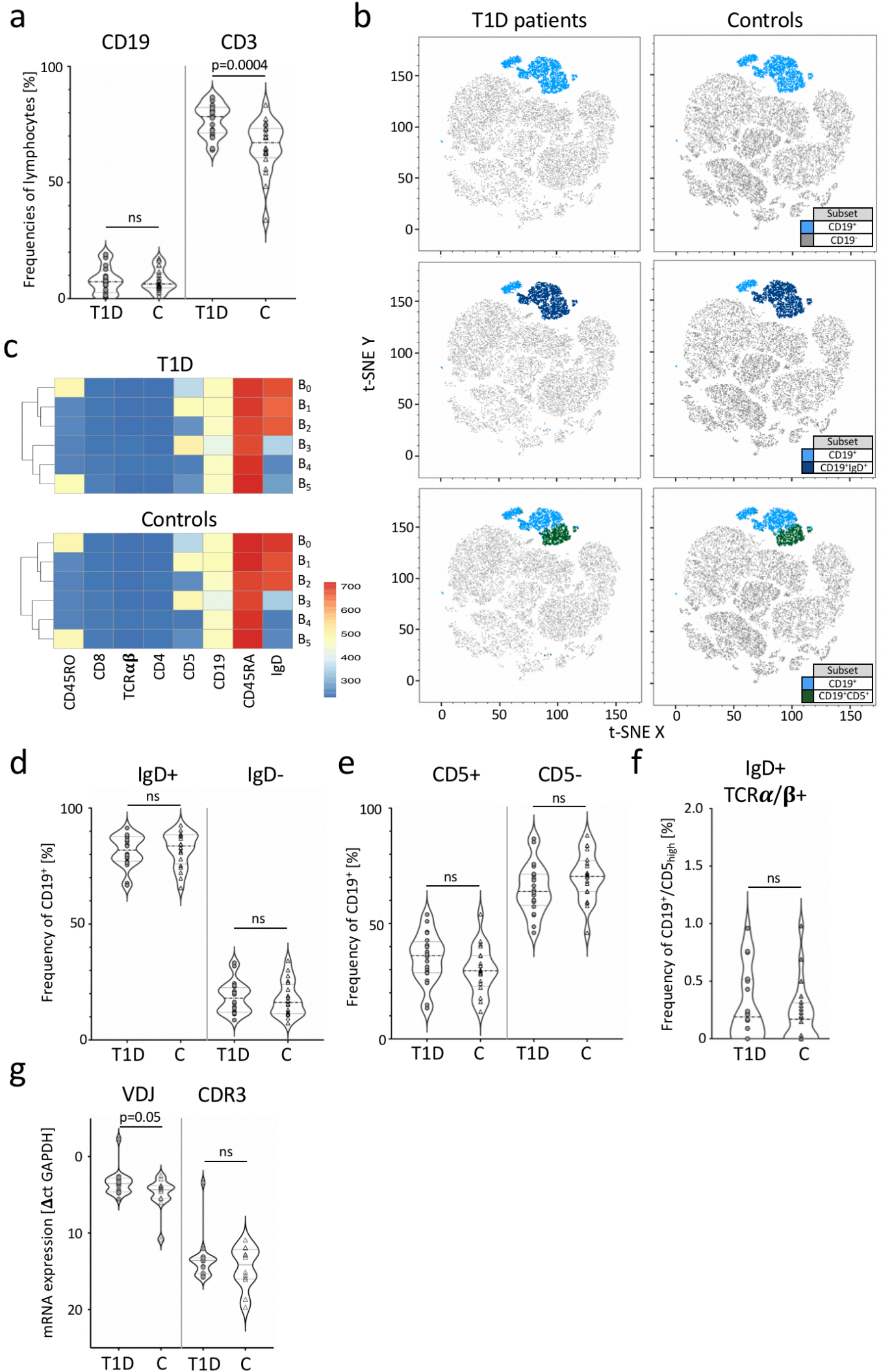
17 performed.

18

19 ***Figure 2: CD8$^+$ T-cells with differential coexpression of CD5 in T1D patients and controls.*** Flow

20 cytometry phenotyping of T-cell subpopulations and analysis by FlowSOM (**a**), TriMAP (**b**),

21 concatenate plots (**c**), and violin graphs of T1D patients and control (**d**) are shown. (**a**)

22 FlowSOM analyses were performed using gated CD3$^+$ T cells of T1D patients and control

23 children separately after concatenation. Seven clusters were chosen arbitrarily and respective

24 CD4$^+$, CD8$^+$ and CD4$^-$/CD8$^-$ (double-negative, DN) clusters are shown for both study groups. (**b**)

25 TriMap zebra plots (including outliers) are generated using a concatenated data set from

1   viable CD3$^+$ T-cell subsets of all individuals (down-sampled 1000 cells per donor sample;

2   triplicate measures per donor were performed). CD8$^+$/CD5$_{low}$ and CD8$^+$/CD5$_{high}$ T cells (see

3   gating in c) are highlighted. (**c**) Gated CD8$^+$ T cells from concatenated CD3$^+$ T cells are shown

4   as smooth density plots including outliers with CD5 expression indicated on the x-axis. Gates

5   were arbitrarily set for CD$_{5low}$, CD5$_{medium}$ and CD5$_{high}$ subset. Respective proportions within

6   concatenated CD8$^+$ T cells are shown for both study groups. (**d**) Violin plots indicate median,

7   25- and 75-percentile values as dotted lines. Nominal p-values of the two-tailed Mann

8   Whitney U-test are given. 20 T1D patients and 20 controls were included and triplicate

9   measures were performed.

10

11   ***Figure 3: CD8$^+$ T-cell proportions with differential CD5 expression are stable in culture and***

12   ***detectable after in vitro T-cell stimulation for 96h.*** Flow cytometry analyses of CD8$^+$ CD5$_{low}$

13   CD5$_{medium}$, and CD5$_{high}$ T-cell subsets *ex vivo* and after 96h *in vitro* culture (**a**) with and without

14   T-cell activation and/or IL-7 stimulation (**b**). (**a**) Pie charts depict proportional distribution of

15   CD8$^+$ T-cell subsets for six healthy donors (HC1 – HC6) *ex vivo* and after 96h *in vitro*. (b)

16   Connected symbol graphs show individual donor proportions of CD5$_{low}$ (upper panel),

17   CD5$_{medium}$ (middle panel), and CD5$_{high}$ (lower panel) CD8$^+$ for 96h *in vitro* non-stimulated vs. IL-

18   7, T-cell activator (CD3/CD28), or combined stimulated samples. Triplicate measures were

19   performed for any condition.
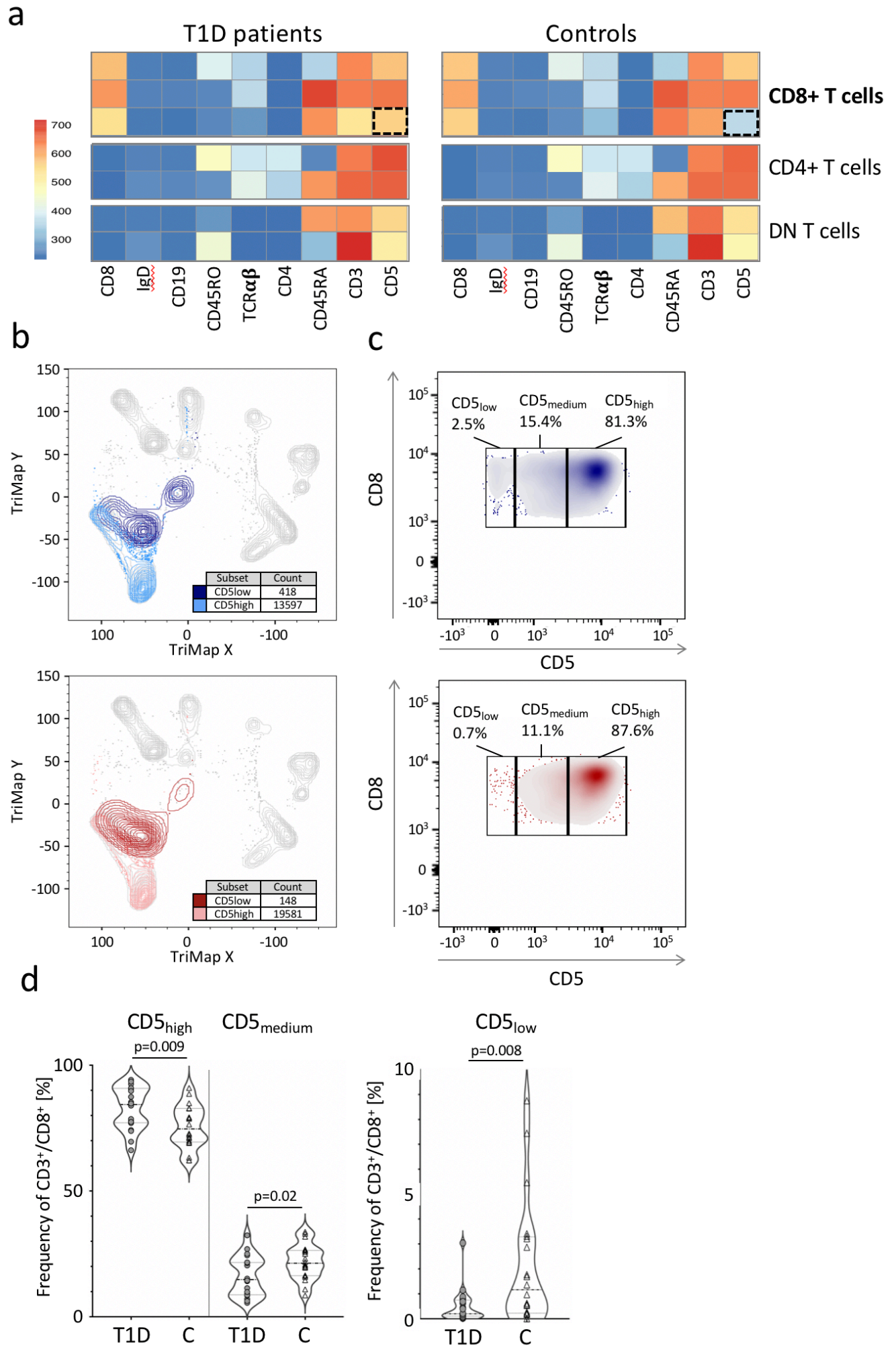
Figure 1

Figure 2

Figure 3